AUTHOR QUERY FORM

ELSEVIER	**Journal:** EA **Article Number:** 19567	**Please e-mail or fax your responses and any corrections to:** **E-mail:** corrections.esch@elsevier.thomsondigital.com **Fax:** +353 6170 9272

Dear Author,

Please check your proof carefully and mark all corrections at the appropriate place in the proof (e.g., by using on-screen annotation in the PDF file) or compile them in a separate list. Note: if you opt to annotate the file with software other than Adobe Reader then please also highlight the appropriate place in the PDF file. To ensure fast publication of your paper please return your corrections within 48 hours.

For correction or revision of any artwork, please consult http://www.elsevier.com/artworkinstructions.

Any queries or remarks that have arisen during the processing of your manuscript are listed below and highlighted by flags in the proof. Click on the 'Q' link to go to the location in the proof.

Location in article	Query / Remark: click on the Q link to go Please insert your reply or correction at the corresponding line in the proof
Q1	Please confirm that given names and surnames have been identified correctly.
Q2	The name of the author in Ref. [25] is different from that mentioned in the text. Please check, and correct if necessary.
Q3	Please note that Refs. [17,53] and [20,54] were identical, and Refs. [53,54] have been deleted. The subsequent references have been renumbered.
Q4	As per the reference style of this journal, all journal references must contain article title. Please check and provide the same.
	Please check this box if you have no corrections to make to the PDF file ☐

Thank you for your assistance.

Electrochimica Acta xxx (2012) xxx–xxx

Contents lists available at SciVerse ScienceDirect

Electrochimica Acta

journal homepage: www.elsevier.com/locate/electacta

Asymmetric hybrid capacitors based on activated carbon and activated carbon fibre–PANI electrodes

Q1 D. Salinas-Torres[a], J.M. Sieben[b], D. Lozano-Castelló[a], D. Cazorla-Amorós[a], E. Morallón[b,*]

[a] Departamento de Química Inorgánica and Instituto Universitario de Materiales, Universidad de Alicante, Ap. 99, Alicante, Spain
[b] Departamento de Química Física and Instituto Universitario de Materiales, Universidad de Alicante, Ap. 99, Alicante, Spain

ARTICLE INFO

Article history:
Received 13 June 2012
Received in revised form
20 September 2012
Accepted 3 November 2012
Available online xxx

Keywords:
Asymmetric supercapacitors
Activated carbon
Polyaniline
Activated carbon fibres

ABSTRACT

Composites consisting of polyaniline (PANI) coatings inside the microporosity of an activated carbon fibre (ACF) were prepared by electrochemical and chemical methods. Electrochemical characterization of both composites points out that the electrodes with polyaniline show a higher capacitance than the pristine porous carbon electrode. These materials have been used to develop an asymmetric capacitor based on activated carbon (AC) as negative electrode and an ACF–PANI composite as positive electrode in H_2SO_4 solution as electrolyte. The presence of a thin layer of polyaniline inside the porosity of the activated carbon fibres avoids the oxidation of the carbon material and the oxygen evolution reaction is produced at more positive potentials. This capacitor was tested in a maximum cell voltage of 1.6 V and exhibited high energy densities, calculated for the unpackaged active materials, with values of 20 W h kg^{-1} and power densities of 2.1 kW kg^{-1} with excellent cycle lifetime (90% during the first 1000 cycles) and high coulombic efficiency.

1. Introduction

Electrochemical energy storage devices such as batteries and supercapacitors have attracted considerable attention from the scientific community due to the rapidly increasing demand of energy from green renewable technologies. Batteries and fuel cells have high energy storage capacity but a relatively low specific power density. On the contrary, the electrochemical capacitors have higher power density and longer lifetime exhibiting high coulombic efficiency, larger current density and fast start-up response, although they have a lower energy density [1,2]. Based on the above considerations, the supercapacitors can be used to deliver a high power demand during a short time, without damaging the power train system, when hybrid-electric and fuel cell vehicles are accelerated and to recover the energy when they are braked [3,4].

Usually, commercial supercapacitors are made of high-surface area activated carbons in various forms and work in a symmetric mode, that is, the same activated carbon is used in the positive and negative electrodes. These devices develop high power densities (typically between 1 and 6 kW kg^{-1}) and specific capacitances between 100 and 250 F g^{-1} but they have a low energy density (typically between 2 and 5 W h kg^{-1}) [5–8]. As a consequence a strong research is being done to develop new materials and configurations to increase their energy density but maintaining or increasing the power density [8–10].

One possibility to increase the energy density of the supercapacitor is to use asymmetric configurations in which different materials are used in each electrode and they are combined allowing an increase in the working voltage [8–10].

Interesting materials to be used as positive electrode in an asymmetric configuration are conducting polymers [11]. Among the conducting polymers, one of the most used is polyaniline (PANI) which presents advantages such as electrical conductivity, electrochemical activity, ease of synthesis and low cost. However, this material presents volume changes, due to the diffusion of ions inside its structure, which confers poor mechanical properties and reduces its cycle stability [11].

A way to improve the performance of PANI would be the use of PANI–carbon composites [11–37] where thin films of the conducting polymer could minimize the negative properties of the bulk material. Most of these studies deal with the polymerization of PANI with carbon nanotubes (single- and multiwalled) and nanofibres [12–17,29,33–37] and there are various papers reporting the synthesis of PANI–carbon composites with carbon materials such as cloths [18], graphene sheets [19,20,30–32], aerogels [21], fibres [22,25] and powdered activated carbon [23,24,26–28].

Polyaniline/porous carbon or PANI/carbon fibre composites were prepared by chemical or electrochemical techniques. These carbon materials provide a large surface for the deposition of PANI, increasing the utilization of the electroactive regions. For instance, Chen and Wen [27] implanted PANI by electro-polymerization on

* Corresponding author.
E-mail address: morallon@ua.es (E. Morallón).

0013-4686/$ – see front matter © 2012 Published by Elsevier Ltd.
http://dx.doi.org/10.1016/j.electacta.2012.11.039

porous activated carbon and obtained a capacitance increase of more than 60% in comparison with the bare carbon electrode. On the other hand, Ryu et al. [24] prepared PANI/carbon composites by chemical polymerization and observed a capacitance increase of about 40% with a PANI content 16 wt.%. However, the specific capacitance decreased when the loading content of PANI on the carbon material further increases. A similar effect was observed by Hu et al. [28] for hierarchical porous carbon/polyaniline composites, although in this case the highest capacitance was obtained with a PANI loaded of 22.4%. Teng et al. [25] obtained a capacitance enhancement of about 50% in comparison with bare carbon. This improvement was reached for a composite with a polymer content lower than 5 wt.%.

Recently, graphene (or graphene oxide) and carbon nanotubes (or nanofibres) have received a fast growing research interest. As a result, composite materials based on nanotubes, nanofibres or graphene sheets and conducting polymers such as PANIs have been tested as supercapacitor electrodes. These composites exhibit high capacitances (higher than the powdered activated carbon/PANI composites) and relative good stability due to the synergetic combination of the good conducting and mechanical properties of carbon materials and high pseudocapacitance of PANI. However, the specific capacitance in these composites is mainly governed by the pseudofaradic process from PANI, since nanotubes, nanofibres and graphene posses low double layer capacitances. Therefore, high capacitances are only obtained with PANI contents between 40 and 70 wt.% [13,15–17,20,30,36,37], which can reduce the cycle life time by degradation problems of PANI composites. In addition, the carbon nanotubes, carbon nanofibres and graphene sheets are still very expensive and difficult to make in large quantities.

Among the different options, the preparation of PANI-based materials in which a thin film of the conducting polymer is deposited on the surface of an appropriate high surface area carbon support, is maybe one of the best solutions. For this purpose, the synthesis conditions and the carbon material have to be carefully selected to create a thin film inside the porosity of the support. This is one important difference compare to most of the papers published to the moment.

Recently, we have prepared activated carbon fibre (ACF)–PANI composites by chemical and electrochemical polymerization where the PANI coating takes place inside the microporosity of the ACF. The distribution of PANI inside the porosity has been demonstrated by microbeam small angle X-ray scattering technique [38]. The use of ACF as carbon support has advantages compared to powder or granular AC because of the smaller tortuosity of networks of porosity in ACF than in AC, which makes the ACF to have a shorter path length for the ions to move than in the case of AC [39–41]. As a consequence, the kinetics of charge and discharge will be higher and will contribute to increase the power of the supercapacitor [41].

In the present work, the behaviour of an asymmetric capacitor has been studied in sulphuric acid solution to high potential window. An ACF–PANI material with the polyaniline deposited inside the microporosity of the activated carbon fibres is used as positive electrode and an activated carbon (AC) with a high surface area and appropriate surface chemistry is the negative electrode in an asymmetric capacitor. The nanometric film of PANI loaded on the surface of the ACF prevents pore blockage, which in turn facilitates the penetration of the electrolyte into the micropores. Furthermore, the cycleability of the capacitor can be enhanced because the mechanical integrity of the polymer is improved by the ACF structure. The two electrode materials have been previously electrochemically characterized in aqueous electrolyte in a three electrode cell and cyclic voltammogram and galvanostatic charge–discharge experiments were done in a two electrode cell to evaluate the properties of the asymmetric capacitor.

2. Experimental

The ACF was provided by Osaka Gas Co. Ltd (A20) and a Spanish anthracite was used as the precursor for the preparation of the activated carbon. Potassium hydroxide, ammonium persulphate, hydrochloric and sulphuric acid, ammonium hydroxide and aniline were from Merck p.a., acetylene black was from Strem Chemicals and binder (polytetrafluoroethylene – PTFE) from Sigma–Aldrich. These were also used as received except aniline which was distilled by refluxing under reduced pressure before use. All solutions were prepared with purified water obtained from an Elga Labwater Purelab system (18.2 MΩ cm).

2.1. Activation process

The activated carbon (AC) has been prepared by chemical activation with KOH using an activating agent:carbon ratio = 3:1 and by heating at 5 °C min^{-1} up to 750 °C; this maximum temperature was kept for 2 h [42]. After, the AC was washed several times with a 5 M HCl solution and with distilled water until free of chloride ions. Finally, the sample was dried at 110 °C for 12 h.

2.2. ACF–PANI preparation

Two different polymerization methods were used for the preparation of the ACF–PANI electrodes [38]:

(i) Chemical polymerization (sample A20_C): previous to the preparation of the composite, the adsorption isotherm in aniline solution on the ACF was obtained. Then, the conditions selected for the preparation of the composite corresponding to a loading of 30 wt.% of aniline in the composite according to the aniline isotherm obtained with the ACF. At these experimental conditions it can be considered that all aniline adsorbed in ACF was polymerized. The composite material was prepared by introducing 600 mg of ACF during 24 h in a 0.02 M aniline solution. After aniline adsorption, the sample was introduced for an hour in an ammonium persulphate solution in 1 M HCl. The oxidant amount was calculated in order to obtain an aniline:ammonium persulphate molar ratio equal to 1:1. A polyaniline coating is then obtained inside the porosity of the carbon material [38]. The composite was washed with 1 M HCl, followed by washing with 1 M ammonia aqueous solution. The material was dried in dynamic vacuum for 24 h. For the electrode preparation, the composite has been mixed with the binder polytetrafluoroethylene (PTFE, 60 wt.%) and acetylene black (Strem Chemicals) in a ratio 80:10:10 wt.%. The total electrode weight used for the measurements was about 40 mg.

(ii) Electrochemical polymerization (sample A20_E): the procedure used is that described in Ref. [24]. This method consists in mixing a paste of the ACF (~3 mg) with the binder (PTFE, 60 wt.%) and the conductivity promoter (acetylene black) in a ratio 80:10:10 wt.%; this mixture was spread and pressed uniformly and thinly with a spatula onto a graphite disk electrode (0.6 cm diameter). After drying, the electrode was placed as the working electrode in a solution of 0.15 M aniline + 1.0 M HCl + 0.5 M KCl and subjected to electro-polymerization using a three electrodes electrochemical cell. A platinum wire was used as counter electrode and a reversible hydrogen electrode (RHE) served as reference electrode. Single potential step from the lower potential of 0.3 V, where no electrode reaction occurred, to an upper potential of 0.75 V, where the polymerization took place, was done for a time until the total charge passed was 0.5 C mg^{-1}. The amount of polyaniline was calculated by subtracting the total weight of the electrode after polymerization

Please cite this article in press as: D. Salinas-Torres, et al., Asymmetric hybrid capacitors based on activated carbon and activated carbon fibre–PANI electrodes, Electrochim. Acta (2012), http://dx.doi.org/10.1016/j.electacta.2012.11.039

Table 1
Porous texture characterization and quantification of surface oxygen groups (TPD experiments, last two columns) of the activated carbon fibre (A20), activated carbon before (AC) and chemically ACF/PANI composite (A20_C).

Sample	BET ($m^2\,g^{-1}$)	V_{DR} N_2 ($cm^3\,g^{-1}$)	V_{DR} CO_2 ($cm^3\,g^{-1}$)	CO ($\mu mol\,g^{-1}$)	CO_2 ($\mu mol\,g^{-1}$)	O ($\mu mol\,g^{-1}$)
AC	2905	1.39	0.72	2817	1035	4887
A20	1660	0.78	0.38	–	–	–
A20_C	925	0.43	0.30	–	–	–

to the mass before polarization. The amount of PANI loaded was around 30 wt.%.

For the characterization of the sample without polyaniline, the electrode was prepared using A20 sample, acetylene black (Strem Chemicals) and binder in a ratio 80:10:10 wt.%, respectively. The total electrode weight used for the measurements was about 40 mg. After that, the electrode was placed in a stainless steel mesh as a current collector. The same procedure has been used for the AC sample.

2.3. Electrochemical characterization

The electrochemical characterization of the different electrodes was done using a standard three electrodes cell configuration. Reversible hydrogen electrode (RHE), immersed in the same solution, was used as reference and a spiral of platinum wire was employed as a counter electrode. 0.5 M H_2SO_4 solution was used as aqueous electrolyte. The measurements were carried out with an EG&G Potentiostat/Galvanostat model 273 controlled by software ECHEM M270 and an Autolab PGSTAT302. The electrochemical behaviour of the different electrodes was assessed by cyclic voltammetry at 5 mV s^{-1} and galvanostatic experiments. The capacitance values were calculated from the interval between 0 and 0.8 V, dividing the imposed current by the slope of the linear chronopotentiograms plot, taking the average value between charge and discharge processes. The capacitance is expressed in F g^{-1} taking into account the weight of the active part of the composite (that is the activated carbon and the PANI).

The capacitors were also done in a two-electrode cell using a sandwich type construction (electrode/separator/electrode) with a glassy fibrous membrane between the electrodes. Gold has been used as current collector and 0.5 M H_2SO_4 solution as electrolyte. Electrode discs with 10 mm diameter and about 0.3 mm thickness were cut from the carbon pastes. The values of specific capacitances were determined by galvanostatic charge/discharge cycling, the current range between 25 and 2000 mA g^{-1} and the capacitance value was estimated from the discharging time and was referred to the total weight of the active mass of both electrodes. The equivalent series resistance (ESR) was obtained from charge–discharge cycles.

2.4. Physicochemical characterization

Porous texture was characterized by physical adsorption of N_2 (–196 °C) and CO_2 (0 °C), using an automatic adsorption system (Autosorb-6, Quantrachrome). The samples were outgassed at 250 °C under vacuum for 4 h. Nitrogen adsorption results were used to determine BET surface area values and Dubinin–Radushkevich (DR) micropore volumes (V_{DR} N_2) as well as the average pore size [43,44]. Narrow micropore volume (pore size < 0.7 nm, approximately) was obtained from CO_2 adsorption data (V_{DR} CO_2) [44]. Table 1 shows the porous texture values obtained for the AC, the activated carbon fibres (A20) and the A20_C samples. Temperature programmed desorption (TPD) experiments were done in a DSC–TGA equipment (TA Instruments, SDT 2960 Simultaneous) coupled to a mass spectrometer (Thermostar, Balzers, GSD 300 T3),

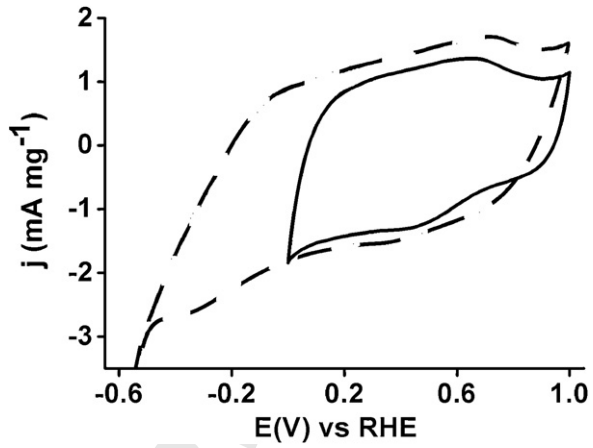

Fig. 1. Steady cyclic voltammograms of AC electrode in 0.5 M H_2SO_4 solution. Scan rate = 5 mV s^{-1}. Three-electrode cell configuration.

to characterize the surface chemistry. In these experiments, 10 mg of the sample was heated up to 950 °C (heating rate 20 °C min^{-1}) under a helium flow rate of 100 ml min^{-1}.

3. Results and discussion

Previous to the study of the asymmetric capacitor, the electrochemical behaviour of the negative and positive electrodes has been performed in a three electrochemical cell.

3.1. Electrochemical characterization of the negative electrode

Fig. 1 shows the voltammetric response of AC electrode in acid medium. The voltammogram between 0 and 1 V exhibits a quasi-rectangular shape, indicating that the main contribution to capacitance is the charge and discharge of the double layer. However, a clear redox process at around 0.65 V during the positive sweep and the counter peak at 0.48 V during the negative sweep is observed, that is associated to surface oxygen groups of the activated carbon that contribute to pseudocapacitance [45]. If the lower potential limit decreases, the hydrogen evolution reaction is not observed on the voltammograms (Fig. 1) up to potentials nearby to –0.6 V indicating a high overpotential for hydrogen evolution reaction for this AC electrode.

The specific capacitance obtained from galvanostatic experiments after five cycles at 25 mA g^{-1} is included in Table 2. Taking into account the results presented in this section, it can be concluded that this material is suitable as negative electrode in an

Table 2
Specific capacitance obtained for all the electrodes by galvanostatic experiments at 25 mA g^{-1} in a three electrode cell 0.5 M H_2SO_4 solution.

Sample	C (F g^{-1})
AC	300
A20	150
A20_C	200
A20_E	240

Please cite this article in press as: D. Salinas-Torres, et al., Asymmetric hybrid capacitors based on activated carbon and activated carbon fibre–PANI electrodes, Electrochim. Acta (2012), http://dx.doi.org/10.1016/j.electacta.2012.11.039

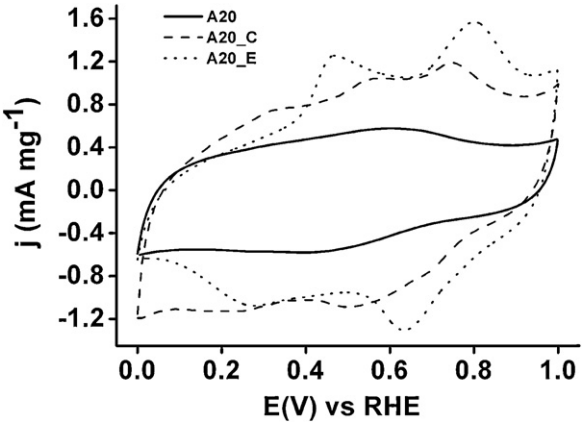

Fig. 2. Steady cyclic voltammograms of A20 (solid line), A20_C (dashed line) and A20_E (dotted line) electrodes in a 0.5 M H_2SO_4 solution. Scan rate was 5 mV s^{-1}. Three-electrode cell configuration.

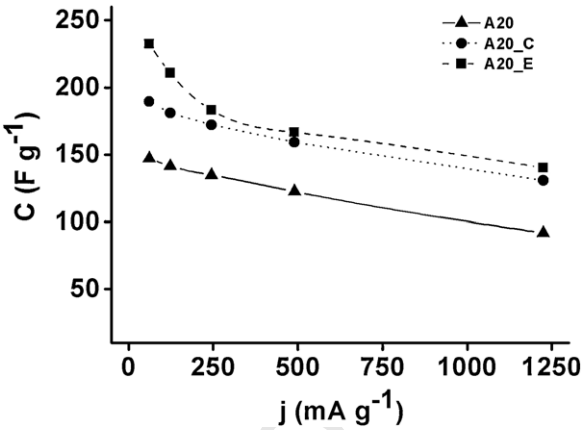

Fig. 3. Specific capacitance at different current densities for A20 and ACF/PANI composites: A20_C and A20_E in 0.5 M H_2SO_4 solution. Three-electrode cell configuration.

asymmetric capacitor due to its high capacitance and high overpotential for hydrogen evolution reaction.

3.2. Electrochemical characterization of the positive electrode

ACF (A20) and their composites with PANI synthesized inside the microporosity of the fibre by chemical (A20_C) and electrochemical (A20_E) methods were characterized by cyclic voltammetry (Fig. 2). For the A20 electrode (solid line) the voltammogram shows a weak peak centred at 0.60 V during the forward scan related to the presence of some surface oxygen groups [45]. The voltammograms for A20_C (dashed line) and A20_E (dotted line) show an increase in the capacitance and the presence of several redox peaks associated to the redox processes of polyaniline. For the A20_E electrode a peak at around 0.45 V appears during the forward voltammetric scan. This peak is associated with the oxidation of emeraldine to leucoemeraldine states of polyaniline, while the anodic peak near 0.8 V can be ascribed to the oxidation of leucoemeraldine to pernigraniline of polyaniline. On the other hand, A20_C electrode shows a voltammogram with some differences compared the one obtained with the A20_E electrode indicating differences in the structure of the polymer. The potential of the redox processes seems to be shifted with respect to those obtained with pure polyaniline. Then, the presence of some defects (generally quinone groups) in the polymer structure as consequence of the overoxidation of polyaniline to potentials higher than 0.9 V cannot be ruled out [26]. These differences could be consequence of the lower amount of sample in the case of electropolymerized sample.

It can be remarked here that the polyaniline film is located inside the porosity of the activated carbon fibre with a thickness around 0.5 nm [38]. This thin film of polyaniline does not impede the entrance and exit of anions inside the porosity of the fibre since the pore size is sufficiently large for the composite [38], but it could prevent the volume change of the electrode during the charge–discharge process what is an important advantage compared to other PANI/carbon composites.

The capacitance values calculated from the galvanostatic experiments for the A20, A20_C and A20_E are included in Table 2. The values measured for the ACF with polyaniline are higher than for the pristine ACF due to the pseudocapacitance behaviour of PANI during the doping/dedoping process.

The evolution of the specific capacitance at different applied currents normalized to the active mass for both composites and the pristine activated carbon fibre (A20) is shown in Fig. 3. It can be observed that the capacitance decreases with the applied current for both composites with a similar trend. Initially, the capacitance value of A20_E is higher than A20_C, but with increasing current density the capacitance values become very close. This loss of capacitance could be related to ion diffusion problems inside the pores at high current densities. It must be remarked that the smaller weight of sample for A20_E has an influence in the rate performance what can explain the better values for this electrode.Interestingly, the slope for the capacitance versus current plot in the higher current region (i.e., above 250 mA g^{-1}), is similar for all samples, which is in agreement with the presence of a thin layer of PANI inside the porosity and a sufficiently large pore size for the composite [38], which would allow a similar rate of ion diffusion within the pores. This result also suggests that the doping/dedoping process of the polymer is a fast process compared to bulk PANI and that it is not slower than the ion diffusion within the porosity.

In view of the above results, A20_E and A20_C composites are interesting materials to be used as positive electrodes and both of them have a similar performance. However, the lower weight of A20_E can lead to an overestimation of their performance, not only because the mass of the active material and thickness of the electrode influences the capacitive behaviour, but also because mass measurement errors can be significant for microgram sized electrodes [46]. In this respect, we have chosen sample A20_C for the asymmetric supercapacitor study, described in the next sections, because the chemical polymerization permits the preparation of higher amounts of material, what is desirable from a practical point of view.

3.3. Optimization of the asymmetric AC/ACF–PANI capacitor

From the previous analysis, it is possible to establish that an asymmetric supercapacitor can be built by the combination of ACF–PANI composite (A20_C) as the positive electrode and the activated carbon (AC) as the negative electrode. In this way, the negative electrode material exhibits a high specific capacitance due to their high surface area and a high overpotential for the hydrogen evolution reaction. On the other hand, the positive electrode material combines a high surface area and the pseudo-faradic contribution of PANI avoiding the problems of bulk polyaniline.

In an asymmetric configuration the two electrodes are materials of different characteristics, so the applied voltage should be distributed between them depending on their capacitance [47,48]. Therefore, before assembling the asymmetric system it is necessary to optimize the mass ratio of the electrodes to improve their performance.

Recently Snook et al. [48] developed simple, but elegant, mathematical expressions that can be employed to optimize the electrode

mass ratios and to maximize the specific energy in asymmetric capacitors based on conducting polymers and activated carbons. The authors obtained an expression capable of estimating the optimum gravimetric mass ratios over a wide range of possible polymer-type electrodes by fixing the capacitance value of an activated carbon electrode, through the following non-linear equation:

$$\gamma_{max} = \left(\frac{C_{(-)}}{C_{(+)}}\right)^{1/2} \quad (1)$$

where γ_{max}, $C_{(-)}$ and $C_{(+)}$ are the maximum value of the mass ratio and the specific capacitances of the negative and positive electrodes, respectively. γ can also be expressed as:

$$\gamma = \frac{m_{(+)}}{m_{(-)}} \quad (2)$$

where $m_{(-)}$ and $m_{(+)}$ are the mass of the active materials in the negative and positive electrodes. From the above relationships the suitable mass ratio coefficient necessary to obtain an asymmetric capacitor with maximum specific energy performance can be calculated. For comparison purposes, the asymmetric capacitor prepared using the raw A20 without polyaniline as positive electrode and the symmetric capacitor with activated carbon (AC) have been also measured. From the capacitance data in Table 2 the gravimetric mass ratio for the AC/A20_C and AC/A20 asymmetric configurations takes values of 1.22 and 1.41, respectively.

Once the mass of the electrodes has been calculated, the asymmetric system will be characterized by charge–discharge experiments at different constant current densities within the potential window of 1.6 V. At this potential window and considering the mass of electrodes calculated from Eq. (2), the theoretical potential swing for the positive and negative electrodes is 55% and 45% respectively for the PANI containing capacitor. This value has been calculated using the equations in Ref. [48].

3.4. Study of the asymmetric AC/ACF–PANI capacitor

After optimizing the parameter commented previously, asymmetric two-electrode capacitors were assembled in 0.5 M H_2SO_4 solution. Fig. 4 shows the voltammograms obtained in a two electrode cell configuration for the asymmetric capacitors for the potential window of 1.6 V before and after 1000 cycles of galvanostatic charge–discharge experiments. The voltammograms of an asymmetric two electrode cell prepared with ACF without polyaniline as positive electrode is also studied, and, for comparison purposes, the voltammogram of the symmetric capacitor prepared with activated carbon is also included. It can be observed, a similar behaviour for asymmetric AC/A20 capacitor and the symmetric AC/AC capacitor, that is a quasi-rectangular shape of the voltammograms at potentials lower than 1.2 V; however, at higher potentials, an oxidation current is observed, being the intensity higher for the AC/A20 capacitor (Fig. 4a). The voltammogram for the asymmetric AC/A20_C shows the redox processes associated with polyaniline and the oxidation current at higher potentials decreases with respect to the AC/A20 capacitor. Then, it seems that polyaniline decreases the oxidation of the A20 sample. The chronopotentiograms at 500 mA g^{-1} for the three capacitors in a potential window of 1.6 V are shown in Fig. 5a. The chronopotentiograms for AC/AC and AC/A20 (Fig. 5a) show a quasi-triangular shape indicating the absence of bulk faradic processes. However, for the asymmetric AC/A20_C capacitor, a slight deviation of this shape is observed as consequence of the pseudofaradic processes of polyaniline. Fig. 5b shows the behaviour of this asymmetric capacitor with current density. It can be observed a good performance until 2 A g^{-1}.

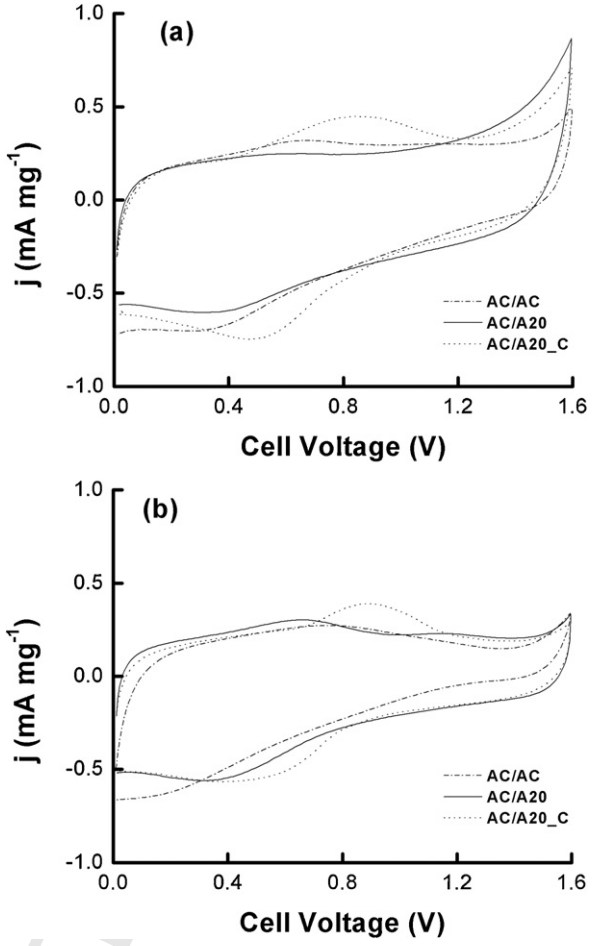

Fig. 4. (a) Steady voltammograms before the galvanostatic charge–discharge experiments for the AC/AC, AC/A20 and AC/A20_C capacitors. (b) Steady voltammograms for the AC/AC, AC/A20 and AC/A20_C after 1000 cycles of charge–discharge at 500 mA g^{-1} in 0.5 M H_2SO_4. Potential window: 1.6 V, scan rate was 5 mV s^{-1}; 0.5 M H_2SO_4.

Fig. 6 shows the capacitance variation for the three capacitors obtained in a two electrode cell from 250 mA g^{-1} to 2000 mA g^{-1} at the potential window of 1.6 V. The values of capacitance for the asymmetric capacitor prepared with ACF with PANI increases around 20% with respect to the capacitor prepared without PANI in the whole range of current. It must be pointed out that in all cases the capacitance decreases when the current density increases probably due to ion diffusion problems. However, this decrease is higher for the symmetric capacitor, and it reaches similar capacitance as the AC/A20 capacitor at 2000 mA g^{-1}. The decrease observed for asymmetric AC/A20_C is around 17% lower than the other capacitors. The slower kinetics for AC electrodes compared to ACF electrodes have been discussed in detail elsewhere [41]. The different pore structure and a higher tortuosity for powdered AC explain this behaviour.These results reveal the important role of PANI in this electrochemical asymmetric system. The presence of the conducting polymer improves the charge transfer and also provides charge through the doping–dedoping redox processes of the polymer, enhancing the electrochemical properties of the composite. Moreover, it decreases the oxidation of carbon material (ACF) and probably the oxygen evolution reaction is produced at more positive potentials because the oxidation of polyaniline is produced before.

Once verified that the asymmetric capacitor assembled with the polyaniline–carbon composite has higher specific capacitances in a wide range of applied currents at 1.6 V, a large number of

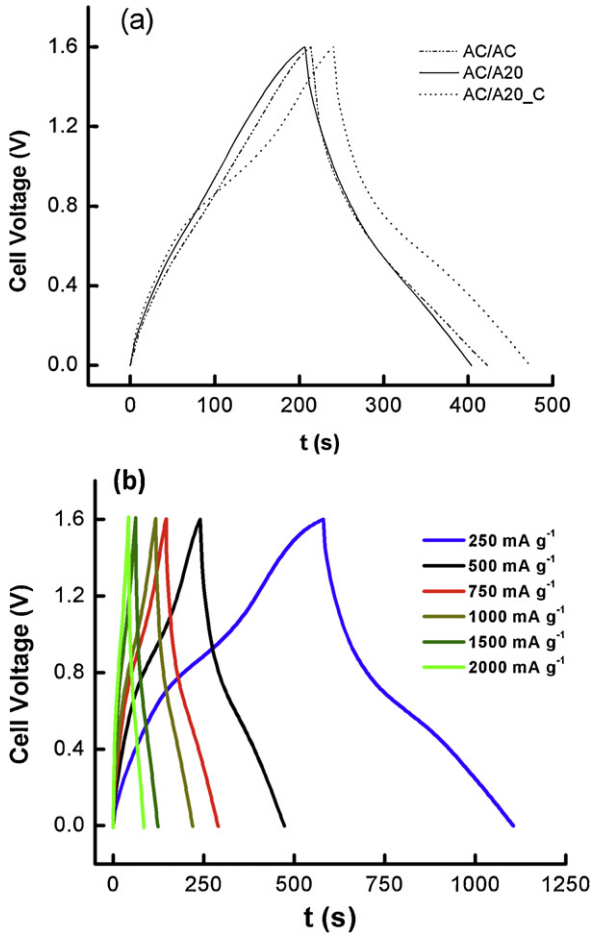

Fig. 5. (a) Chronopotentiograms for the AC/AC, AC/A20 and AC/A20_C capacitors at 500 mA g^{-1}. (b) Chronopotentiograms for AC/A20_C capacitor at different current density. Two-electrode cell configuration; 0.5 M H_2SO_4.

galvanostatic charge–discharge cycles have been performed. The other two capacitors have been also studied for comparison purposes. As it has been commented before for the PANI-containing capacitor, the chronopotentiograms at both potential windows have a quasi linear shape, the coulombic efficiency is above 99%

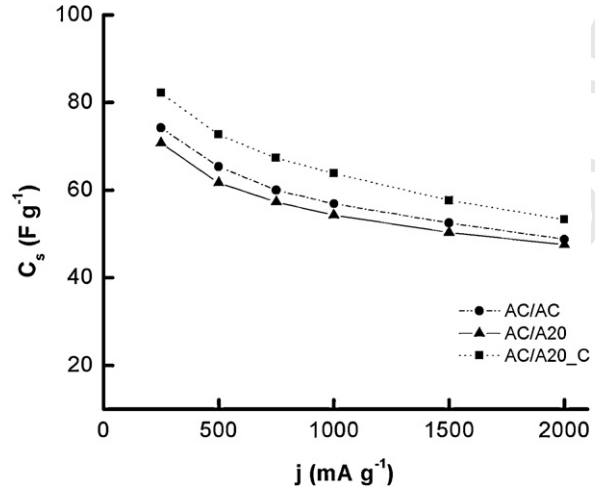

Fig. 6. Capacitance (5 cycles of galvanostatic charge–discharge) variation with increase of current density for AC/AC, AC/A20 and AC/A20_C capacitors operated at 1.6 V window. Two-electrode cell configuration; 0.5 M H_2SO_4.

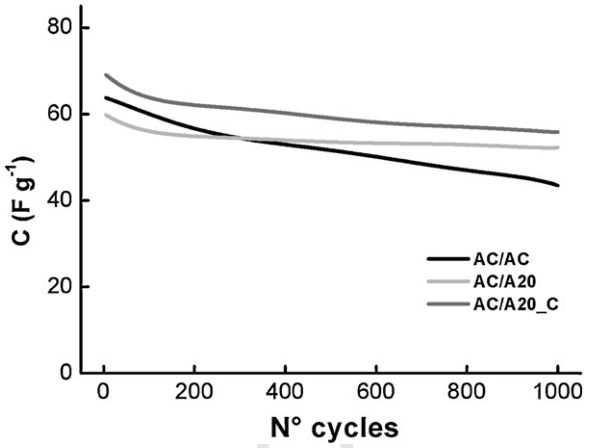

Fig. 7. Evolution of the specific capacitance versus the number of cycles for the AC/AC, AC/A20 and AC/A20_C capacitors at 1.6 V in 0.5 M H_2SO_4. Charge/discharge current density 500 mA g^{-1}. Two-electrode cell configuration.

after 1000 cycles and no additional faradic reaction, such as hydrogen evolution or oxygen evolution, has a significant contribution in the process.

Fig. 7 shows the evolution of the specific capacitance for the three capacitors studied versus the number of galvanostatic cycles. The theoretical capacitance value at 500 mA g^{-1} calculated using gravimetric mass ratio [48] is 52 F g^{-1} and 61 F g^{-1} for AC/A20 and AC/A20_C respectively. The specific capacitance of the asymmetric capacitor AC/A20_C decreases with the number of cycles but the systems retain more than 80% of the initial capacitance (55.3 F g^{-1} in gravimetric basis and 16.1 F cm^{-3} in volumetric basis, calculated using the density of the two electrodes and the membrane) after 1000 cycles at 1.6 V, what is a remarkable result. The largest decrease in capacitance is observed for the symmetric capacitor.

Fig. 4b shows the voltammograms of the two electrode cell capacitors after 1000 cycles at 1.6 V. It can be observed that the voltammogram for the PANI containing capacitor maintains its shape and degradation of the polyaniline is not important. However, for the other two capacitors there is an important change, especially at high potentials for the symmetric capacitor indicating the worse performance in comparison to AC/A20_C capacitor and the significant degradation of the positive electrode after 1000 cycles.

In order to complete the information on the performance of the asymmetric capacitor, the specific power and energy have been calculated. The specific power was determined according to Eq. (3) [5,49]:

$$P_{max} = \frac{V_{max}^2}{4\,ESR\,m_t} \quad (3)$$

where *ESR* is the equivalent series resistance determined from ohmic drop in the charge–discharge measurements (Fig. 5) and m_t is the total active mass of the capacitor.

Additionally, the amount of electrical energy accumulated in the capacitors, which is associated with the capacitance and the voltage window, can be estimated according to the following expression:

$$E = \frac{1}{2}CV^2 \quad (4)$$

Table 3 summarizes the values of energy density for the unpackaged-active material (E), energy density calculated from the theoretical capacitance (E_{calc}) and the maximum power density (P_{max}) obtained for symmetric capacitor, both AC/A20 and AC/A20_C asymmetric capacitors. Interestingly, the values of E are close to those calculated using the theoretical capacitance values

Table 3
Power density and energy density obtained for the capacitors at a potential window of 1.6 V in 0.5 M H_2SO_4 as electrolyte.

Device	P_{max} (kW kg^{-1})	P_{max} (kW dm^{-3})	E (W h kg^{-1})	E (W h dm^{-3})	E_{calc} (W h kg^{-1})
AC/AC	0.5	0.1	15.3	2.2	26.7
AC/A20	1.7	0.3	18.1	2.7	18.2
AC/A20_C	2.1	0.6	20.0	5.7	21.4

(E_{calc}) for the asymmetric capacitors (Table 3), what corroborates the correct design of the capacitor. It can be observed from Table 3 that the specific power values of all the studied capacitors are typical for supercapacitors, and the presence of polyaniline increases around 20% the energy density and 25% the power of the capacitor.

Some values of energy and power densities of unpackaged-advanced electrochemical capacitors using activated carbon as electrodes were reported by Simon and Burke [50]. These electrochemical capacitors are capable of delivering specific energies between 1.7 for a AC Carbon/AC Carbon capacitor in sulfuric acid and 18 W h kg^{-1} for AC Carbon/Graphitic carbon in organic electrolyte and power densities of 1.2 for a AC Carbon/AC Carbon capacitor in sulfuric acid and 6.4 kW kg^{-1} for AC Carbon/Graphitic carbon in acetonitrile as the electrolyte. Interestingly, the values obtained in the asymmetric AC/A20_C capacitor are similar to that obtained in the case of using organic electrolyte and higher than those developed in the case of sulfuric acid electrolyte. Furthermore, values reached with the AC/A20_C arrangement are higher than those reported for several PANI and PANI/carbon composite based systems [51,52,17,20]. However, these results must be put in context because the performance of a capacitor depends on numerous parameters such as architecture of the cell, potential window, mass of the dead components, and electrode thickness [46]. Then, the comparison with data in the literature is not straightforward.

In view of the results, the PANI coating inside the microporosity of the activated carbon fibres enhances power and specific energy of the asymmetric devices, due to its doping/dedoping processes that increase the capacitance of the positive electrode and avoiding the oxidation of the carbon support in the potential window used and probably the oxygen evolution reaction is produced at more positive potentials. In addition, PANI may act as a molecular wire, enhancing the electrochemical performance of the asymmetric supercapacitor.

4. Conclusions

An asymmetric capacitor consisting on ACF with PANI inside its microporosity as positive electrode and a high surface area AC as negative electrode has been designed and tested in acid aqueous solution. These capacitors exhibit higher specific capacitance than that prepared with the pristine ACF material due to the contribution of pseudocapacitance of the polymer coating to the total capacitance and the oxidation of carbon material decreases in the potential window of 1.6 V in sulphuric solution. Moreover, it can be considered that the oxygen evolution reaction is probably produced at more positive potentials.

The asymmetric supercapacitor assembled using the composite ACF–PANI prepared by chemical polymerization as the positive electrode and the porous activated carbon as the negative electrode, generates energy densities of 20 W h kg^{-1} and power densities of 2.1 kW kg^{-1} in cell voltage windows of 1.6 V using an acid aqueous electrolyte. In addition, the asymmetric capacitor shows a good cycling behaviour after the first 1000 charge–discharge cycles at 500 mA g^{-1}. These are very interesting and promising results that will be completed by analysing different electrolytes and longer cycling life tests.

Acknowledgements

Financial support by the Ministerio de Ciencia e Innovación (MAT2010-15273 and CTQ2009-10813) and Generalitat Valenciana and FEDER (PROMETEO/2009/047 and ACOMP/2012/133) projects are gratefully acknowledged. J.M.S. thanks Ministerio de Educación (SB2010-132). D.S.T. thanks Ministerio de Ciencia e Innovación (BES-2010-035238).

References

[1] M. Winter, R.J. Brodd, Chemical Reviews 104 (2004) 4245.
[2] B.E. Conway, Electrochemical Supercapacitors, Kluwer Academic, Plenum Publishers, New York, 1999.
[3] A. Chu, P. Braatz, Journal of Power Sources 112 (2002) 236.
[4] E. Faggioli, P. Rena, V. Danel, X. Andrieu, R. Mallant, H. Kahlen, Journal of Power Sources 84 (1999) 261.
[5] A.G. Pandolfo, A.F. Hollenkamp, Journal of Power Sources 157 (2006) 11.
[6] E. Frackowiak, F. Béguin, Carbon 39 (2001) 937.
[7] M. Inagaki, H. Konno, O. Tanaike, Carbon 195 (2010) 7880.
[8] K. Naoi, P. Simon, Interface (The Electrochemical Society) 17 (2008) 34.
[9] D. Bélanger, T. Brousse, J.W. Long, Interface (The Electrochemical Society) 17 (2008) 49.
[10] J.W. Long, D. Bélanger, T. Brousse, W. Sugimoto, M.B. Sassin, O. Crosnier, MRS Bulletin 36 (2011) 513.
[11] G.A. Snook, P. Kao, A.S. Best, Journal of Power Sources 186 (2011) 1.
[12] H. Mi, X. Zhang, S. An, X. Ye, S. Yang, Electrochemistry Communications 9 (2007) 2859.
[13] C. Meng, C. Liu, S. Fan, Electrochemistry Communications 11 (2009) 186.
[14] M. Wu, G.A. Snook, V. Gupta, M. Shaffer, D.J. Fray, G.Z. Chen, Journal of Materials Chemistry 15 (2005) 2297.
[15] V. Gupta, N. Miura, Journal of Power Sources 157 (2006) 616.
[16] S.R. Sivakkumar, W.J. Kim, J.A. Choi, D.R. MacFarlane, M. Forsyth, D.W. Kim, Journal of Power Sources 171 (2007) 1062.
[17] C. Meng, C. Liu, L. Chen, C. Hu, S. Fan, Nano Letters 10 (2010) 4025.
[18] Y.Y. Horng, Y.C. Lu, Y.K. Hsu, C.C. Chen, L.C. Chen, K.H. Chen, Journal of Power Sources 195 (2010) 4418.
[19] K. Zhang, L.L. Zhang, X.S. Zhao, J. Wu, Chemistry of Materials 22 (2010) 1392.
[20] Q. Wu, Y. Xu, Z. Yao, A. Liu, G. Shi, ASC Nano 4 (2010) 1963.
[21] H. Talbi, P.E. Just, L.H. Dao, Journal of Applied Electrochemistry 33 (2003) 465.
[22] Y.R. Lin, H. Teng, Carbon 41 (2003) 2865.
[23] M.J. Bleda-Martínez, E. Morallón, D. Cazorla-Amorós, Electrochimica Acta 52 (2007) 4962.
[24] K.S. Ryu, Y.G. Lee, K.M. Kim, Y.J. Park, Y.S. Hong, X. Wu, M.G. Kang, R.Y. Song, J.M. Ko, Synthetic Metals 153 (2005) 89.
[25] C.P. Fonseca, D.A.L. Almeida, M.R. Baldan, N.G. Ferreira, Chemical Physics Letters 511 (2011) 73.
[26] M.J. Bleda-Martínez, C. Peng, S. Zhang, G.Z. Chen, E. Morallón, D. Cazorla-Amorós, Journal of the Electrochemical Society 155 (2008) A672.
[27] W. Chen, T. Wen, Journal of Power Sources 117 (2003) 273.
[28] J. Hu, H. Wang, X. Huang, Electrochimica Acta 74 (2012) 98.
[29] S.C. Canobre, D.A.L. Almeida, C.P. Fonseca, S. Neves, Electrochimica Acta 54 (2009) 6383.
[30] F. Chen, P. Liu, Q. Zhao, Electrochimica Acta 76 (2012) 62.
[31] K.S. Kim, S.J. Park, Electrochimica Acta 56 (2011) 6547.
[32] C. Li, G. Shi, Electrochimica Acta 56 (2011) 10737.
[33] K.S. Kim, S.J. Park, Electrochimica Acta 56 (2011) 1629.
[34] M. Yang, B. Cheng, H. Song, X. Chen, Electrochimica Acta 55 (2010) 7021.
[35] H. Zhang, G. Cao, W. Wang, K. Yuan, B. Xu, W. Zhang, J. Cheng, Y. Yang, Electrochimica Acta 54 (2009) 1153.
[36] Y. Zhou, Z.Y. Qin, L. Li, Y. Zhang, Y.L. Wei, L.F. Wang, M.F. Zhu, Electrochimica Acta 55 (2010) 3904.
[37] Z. Zhu, G. Wang, M. Sun, X. Li, C. Li, Electrochimica Acta 56 (2011) 1366.
[38] D. Salinas-Torres, J.M. Sieben, D. Lozano-Castello, E. Morallón, M. Burghammer, C. Riekel, D. Cazorla-Amorós, Carbon 50 (2012) 1051.
[39] G.J. Wilson, M.G. Looney, A.G. Pandolfo, Synthetic Metals 160 (2010) 655.
[40] M. Suzuki, Carbon 32 (1994) 577.
[41] M.J. Bleda-Martínez, D. Lozano-Castelló, D. Cazorla-Amorós, E. Morallón, Energy & Fuels 24 (2010) 3378.
[42] D. Lozano-Castelló, M.A. Lillo-Ródenas, D. Cazorla-Amorós, A. Linares-Solano, Carbon 39 (2001) 741.
[43] F. Stoeckli, L. Ballerini, Fuel 70 (1991) 557.

[44] D. Cazorla-Amorós, J. Alcañiz-Monge, M.A. de la Casa-Lillo, A. Linares-Solano, Langmuir 14 (1998) 4589.
[45] M.J. Bleda-Martínez, D. Lozano-Castelló, E. Morallón, D. Cazorla-Amorós, A. Linares-Solano, Carbon 44 (2006) 2642.
[46] M.D. Stoller, R.S. Ruoff, Energy & Environmental Sciences 3 (2010) 1294.
[47] V. Khomenko, E. Raymundo-Piñero, F. Béguin, Journal of Power Sources 153 (2006) 183.
[48] G.A. Snook, G.J. Wilson, A.G. Pandolfo, Journal of Power Sources 186 (2009) 216.
[49] V. Khomenko, E. Raymundo-Piñero, F. Béguin, Journal of Power Sources 195 (2010) 4234.
[50] P. Simon, A. Burke, Interface (The Electrochemical Society) 17 (2008) 38.
[51] F. Fusalba, P. Gouérec, D. Villers, D. Bélanger, Journal of the Electrochemical Society 148 (2001) A1.
[52] J.H. Park, O.O. Park, Journal of Power Sources 111 (2002) 185.

Please cite this article in press as: D. Salinas-Torres, et al., Asymmetric hybrid capacitors based on activated carbon and activated carbon fibre–PANI electrodes, Electrochim. Acta (2012), http://dx.doi.org/10.1016/j.electacta.2012.11.039